

2022

Pressure Drop of Low GWP Refrigerant Mixture of R1234yf and R32 inside Small Diameter Horizontal Microfin Tube

Hakimatul Ubudiyah

Afdhal Kurniawan Mainil

Kazuki Sadakata

Keishi Kariya

Akio Miyara

Follow this and additional works at: <https://docs.lib.purdue.edu/iracc>

Ubudiyah, Hakimatul; Mainil, Afdhal Kurniawan; Sadakata, Kazuki; Kariya, Keishi; and Miyara, Akio, "Pressure Drop of Low GWP Refrigerant Mixture of R1234yf and R32 inside Small Diameter Horizontal Microfin Tube" (2022). *International Refrigeration and Air Conditioning Conference*. Paper 2362. <https://docs.lib.purdue.edu/iracc/2362>

This document has been made available through Purdue e-Pubs, a service of the Purdue University Libraries. Please contact epubs@purdue.edu for additional information. Complete proceedings may be acquired in print and on CD-ROM directly from the Ray W. Herrick Laboratories at <https://engineering.purdue.edu/Herrick/Events/orderlit.html>

Pressure Drop of Low GWP Refrigerant Mixture of R1234yf and R32 inside Small Diameter Horizontal Microfin Tube

Hakimatul UBUDIYAH^{1*}, Afdhal Kurniawan MAINIL¹, Kazuki SADAKATA¹, Keishi KARIYA²,
Akio MIYARA^{2,3}

¹Graduate School of Science and Engineering, Saga University
Saga, Japan
Phone: +81-80-9673-1246, E-mail: hakimatulubudiyah@gmail.com

²Department of Mechanical Engineering, Saga University,
Saga, Japan
Phone: +81-952-28-8623, Fax: +81-952-28-8587, E-mail: miyara@me.saga-u.ac.jp

³International Institute for Carbon-Neutral Energy Research, Kyushu University,
Fukuoka, Japan

* Corresponding Author

ABSTRACT

The use of R32, which has a GWP of 675 and an ODP of 0, is increasing. However, the GWP of R32 is not low enough to satisfy the Kigali amendment, though the GWP is relatively lower than other HFCs. On the other hand, research attention has been focused on R1234yf because its thermophysical properties are close to R134a and its GWP is lower than 1. But, due to its limited thermophysical properties, R1234yf is not a suitable replacement for R32. One solution is to use refrigerant combinations with a lower GWP and higher performance, such as R1234yf and R32. This paper showed the pressure drop characteristics of the low GWP zeotropic refrigerant mixture R1234yf/R32 inside a horizontal microfin tube (equivalent diameter of 3.18 mm). The experiments were carried out at saturation temperatures of 20°C and 30°C, vapor quality ranging from 0 to 1, and mass velocity ranging from 50 kg m⁻²s⁻¹ to 200 kg m⁻²s⁻¹. The effect of saturation temperature, vapor quality, and mass velocity on pressure drop was presented. Along with mass velocity and vapor quality increments, the pressure drops of refrigerant mixtures increased. In contrast, the pressure drop decreased along with the increase in saturation temperature. The measured pressure drop was compared to a correlation.

1. INTRODUCTION

Refrigeration, along with spaceflight, the internet, and computers, is regarded as one of the most significant achievements of the 20th century (Constable and Somerville, 2003). Refrigeration and air conditioning consume approximately 20% of all energy consumed globally (McLinden and Huber, 2020). One device that uses refrigerant to operate is the air conditioning unit. By 2020, the world's air conditioning units are expected to number 1.9 billion. The United States, China, Japan, and South Korea account for the majority of these.

So far, R410A is the dominant refrigerant used in domestic air conditioners. Even though this refrigerant does not contribute to the depletion of the ozone layer, it has a high global warming potential (GWP) of 1924 (Myhre *et al.*, 2013). Research efforts have been concentrated on creating lower GWP alternative refrigerants and decreasing the quantity of refrigerant charge in HVAC&R systems to decrease its influence on global warming (Poggi *et al.*, 2008). The most relevant chemical companies are developing alternatives to R410A as a result of the recently imposed limits (Oruç *et al.*, 2018). This option should be chosen based on a variety of variables, including low environmental degradation, safety, and adaptability to operating temperatures (McLinden *et al.*, 2014).

Recently, R32 has been used in domestic air conditioners as a substitute for R410A, and almost 40% of room air conditioning in Japan uses it as the refrigerant (Vuppaladadiyam *et al.*, 2022). However, since the Kigali Amendment mandated that the use of HFCs should be reduced dramatically over the next few decades to avoid an increase in global average temperature of 0.5 °C by 2100, the global warming potential (GWP) of R32 is not low enough to meet the Amendment.

On the other hand, research attention has been focused on R1234yf (Del Col *et al.*, 2010; Diani *et al.*, 2014, 2017) because its thermophysical properties are close to R134a and its GWP is lower than 1. But, due to its limited thermophysical properties, R1234yf is not a suitable replacement for R32. One solution is to use refrigerant combinations between R1234yf and R32 to get the higher performance. Not only to enhance the heat transfer performance but also to minimize the pressure loss of the system. Hence, more studies are needed to analyze the performance of the mixture refrigerant.

Another factor that affects the heat transfer enhancement is the use of small-diameter tubes. The use of a small diameter microfin tube ($do = 5\text{-}2.5$ mm) presents a very good potential for refrigerant charge minimization. Additionally, a small-diameter microfin tube could reduce the heat exchanger's weight and cost. Therefore, in this study, we investigated the pressure drop of a low GWP refrigerant mix of R1234yf and R32 inside a small-diameter horizontal microfin tube. In this paper, the effect of saturation temperature, vapor quality, and mass velocity on pressure drop was presented.

2. EXPERIMENTAL SETUP

The description of experimental apparatus and test section details are shown in the Figure 1 and 2. Figure 1 shows the details of the experimental apparatus and its components. There are 2 main loops in the apparatus: the refrigerant loop and the water loop. The pump pumps the liquid refrigerant through the control valve, Coriolis flow meter, mixing chamber, preheater, and to the test section. Then, refrigerant from the test section is pumped out through the accumulator and is cooled by the cooler. After that, refrigerant is pumped again through the test section.

There are 2 pumps in this experimental apparatus, one for the low mass flow ($50 \text{ kg m}^{-2}\text{s}^{-1}$) and the other for the high mass flow (larger than $50 \text{ kg m}^{-2}\text{s}^{-1}$). This apparatus also connected to a PC using a multimeter to collect all the measurement signal. Gas chromatograph is connected to the apparatus to measure the composition of mixture refrigerant. R454B with mass composition of 68.9 % R32 and 31.1 % R1234yf was charged, measured average composition was 70.8 % R32 and 29.2 % R1234yf.

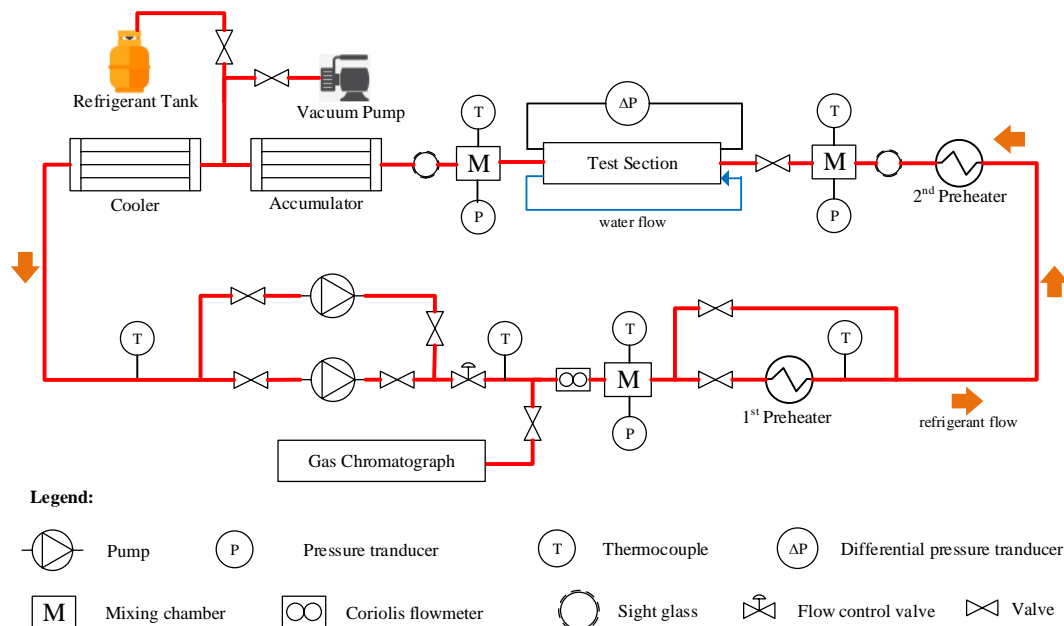


Figure 1: Experimental Apparatus

Figure 2 shows the details of the test section. The test tube is a microfin tube with a 3.18 mm equivalent diameter. The total length of the tube is 852 mm, and the effective length of heat transfer is 744 mm. The temperature of the test section's wall is measured using 12 T-type thermocouples integrated into the data logger. The test tube has a 0.15 mm thick wall (δ), a 0.10 mm fin height, a 10° helix angle (θ), a 33° apex angle (γ), and 25 fins. The experiments are conducted at mass velocity ranging from 50 to 200 $\text{kgm}^{-2}\text{s}^{-1}$, with saturation temperatures ranging from 20°C to 30°C and vapor quality ranging from 0 to 1.

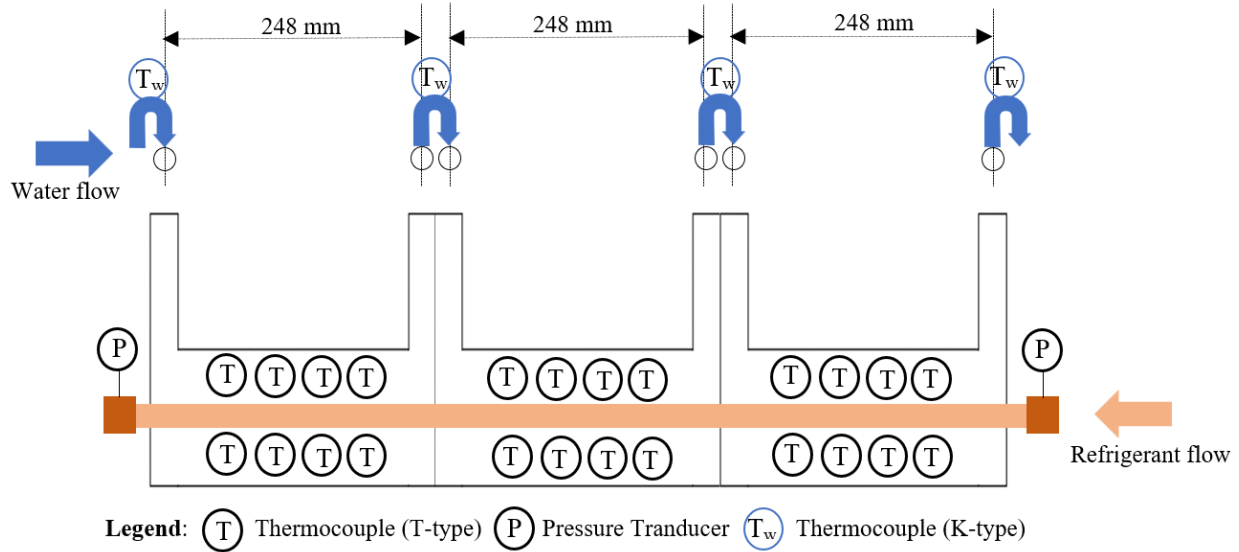


Figure 2: Test Section Details

3. DATA REDUCTION

Some terms are used to estimate the total pressure drop (ΔP_T) of a fluid inside a tube. Frictional pressure drops (ΔP_F), gravitational pressure drops, momentum pressure drops, and minor pressure drops due to flow disturbance are the most common terms. Because the test section position is horizontal and the test mode is adiabatic in this study, the gravitational and momentum pressure drop terms are zero. However, a minor pressure drop is considered as a result of the test section's sudden contraction (ΔP_c) and expansion (ΔP_e) at the inlet and outlet headers, respectively. As a result, the total two-phase pressure drop term is:

$$\Delta P_T = \Delta P_F + \Delta P_c + \Delta P_e \quad (1)$$

In the case of sudden contraction and expansion pressure drops, it is estimated by Equation (2) and Equation (3), respectively, according to Collier and Thome (1994) correlation.

$$\Delta P_c = \frac{G^2 v_l}{2} \left[\left(\frac{1}{C_c} - 1 \right)^2 + \left(1 - \frac{1}{\delta^2} \right) \right] \left[1 + \left(\frac{\Delta v_v}{v_l} \right) x \right] \quad (2)$$

$$\Delta P_e = G^2 \delta_e (1 - \delta_e) v_l \left[\frac{(1-x)^2}{1-\xi} + \left(\frac{v_v}{v_l} \right) \frac{x^2}{\xi} \right] \quad (3)$$

Where G is the mass velocity, C_c is the coefficient of contraction, δ is the area ratio, v_l is liquid specific volume, v_v is vapor specific volume, and ξ is void fraction. In addition, the void fraction ξ is assumed to be constant due to the homogeneous model.

The vapor quality is expressed by Equation (4), and local enthalpy is expressed by Equation (5).

$$x_{(i)} = \frac{h_{(i)} - h_l}{h_v - h_l} \quad (4)$$

$$h_{(i)} = h_{in,preheater} + \left(\frac{Q}{G}\right) \quad (5)$$

Where Q is amount of heat supplied by the electricity into the preheater, and mass velocity (G) is calculated by Equation (6).

$$G = \frac{m_R}{A} \quad (6)$$

In this study, the tube used is a microfin tube, so equivalent diameter (d_{eq}) is used for the calculation, and it is expressed by Equation (7).

$$d_{eq} = \sqrt{\frac{4A}{\pi}} \quad (7)$$

Where A is the cross-sectional area, and it is expressed by Equation (8).

$$A = \frac{\pi}{4} (\text{Fin bottom inner diameter})^2 - \text{total area of fin} \quad (8)$$

4. EXPERIMENTAL RESULTS AND ANALYSIS

This section presents the effect of mass velocity, vapor quality, and saturation temperature on frictional pressure drop. Figure 3 and 4 show the relation between the frictional pressure drop $\Delta P_F / \Delta Z$ and the vapor quality. The comparison between the predicted and experimental data also can be seen at figure 5.

Figure 3 shows the effect of mass velocity and vapor quality on frictional pressure drop at saturation temperature of 20°C. Along with the increase in mass velocity, frictional pressure drop increases as expected. This is because the shear stress and interfacial friction between vapor-liquid two-phase flow in the tube increase, and it is attributable to the increase in pressure with mass velocities. The highest pressure drop is found at the highest mass velocity, at 200 kg m⁻²s⁻¹. (Khairul Bashar *et al.*, 2020) and (Hirose *et al.*, 2018) also found the same phenomena about the increase in frictional pressure drop along with the mass velocity and vapor quality.

Figure 4 shows the frictional pressure drop versus vapor quality at saturation temperature 20°C and 30°C. Under the identical operating parameters of vapor quality and mass velocity, the pressure drop at a saturation temperature of 30°C is lower than the pressure drop at a saturation temperature of 20°C. It can be explained by examining the refrigerant's thermophysical properties at various saturation temperatures, such as liquid density and viscosity. At saturation temperature, 30 °C, liquid density and viscosity are lower, resulting in lower fluid velocity.

Figure 5 shows the comparison between the predicted and experimental frictional pressure drop of R454B mixtures using the Goto *et al.* (2001) correlation, Equation (9). The data of experimental and predicted frictional pressure drop is shown in Appendix Table 1. From the figure, it can be seen that the predicted values are well predicted for all of mass velocity, with average deviation (AD) of -32% and mean absolute deviation (MD) of 32%. The average deviation and mean deviation are calculated by Equation (10) and Equation (11), respectively.

$$\left(\frac{\Delta P}{\Delta Z}\right)_F = \phi_v^2 \left(\frac{\Delta P}{\Delta Z}\right)_v \tag{9}$$

$$AD = \frac{1}{n} \sum_{i=1}^n \left(\frac{\Delta P_{pre} - \Delta P_{exp}}{\Delta P_{exp}} \right) \times 100 \tag{10}$$

$$MD = \frac{1}{n} \sum_{i=1}^n \left| \frac{\Delta P_{pre} - \Delta P_{exp}}{\Delta P_{exp}} \right| \times 100 \tag{11}$$

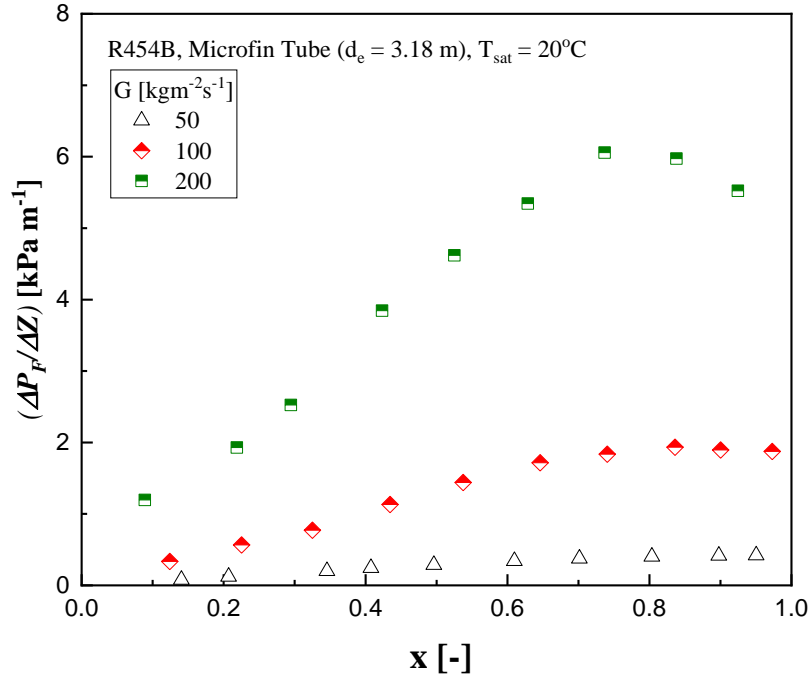


Figure 3: Effect of mass velocity and vapor quality on frictional pressure drop

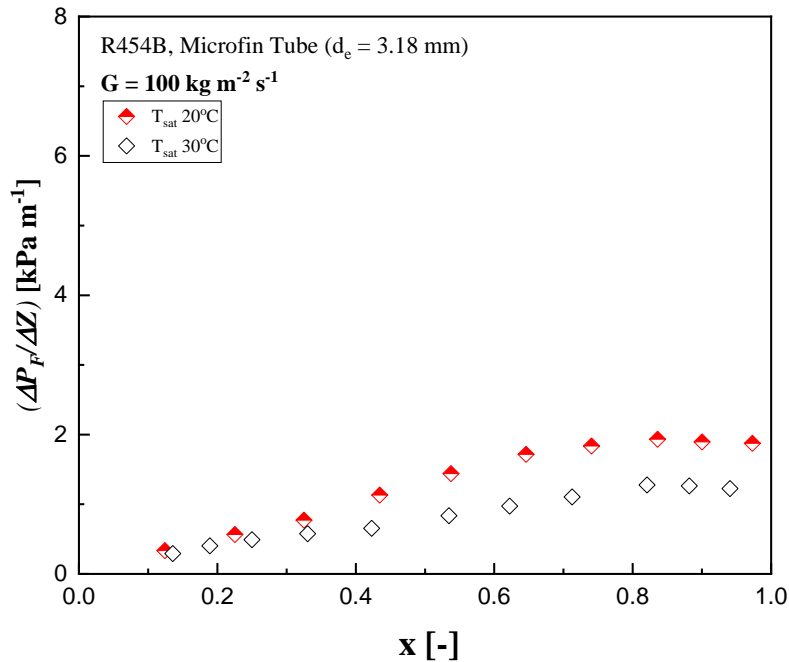


Figure 4: Effect of saturation temperature on frictional pressure drop

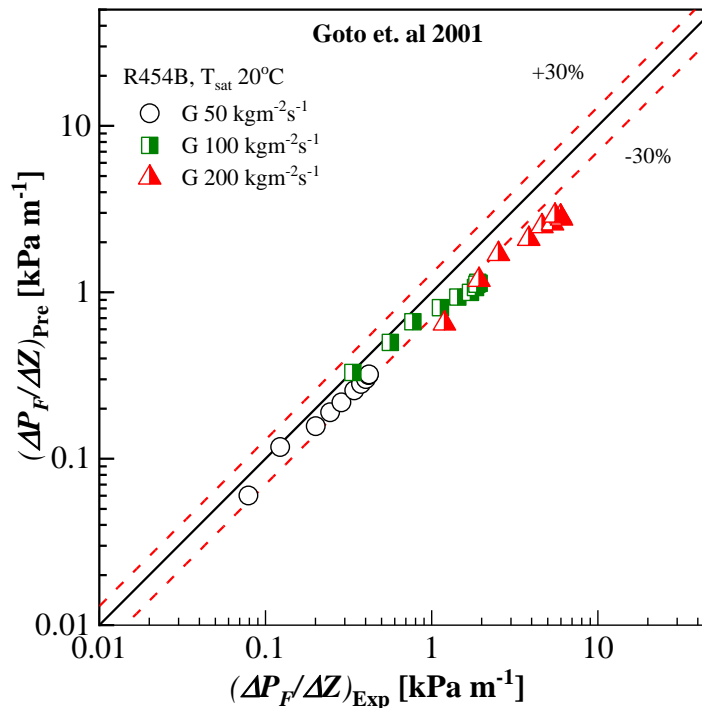


Figure 5: Comparison of experimental pressure drop and predicted pressure drop

5. CONCLUSIONS

In this study, the pressure drop of a low GWP refrigerant mixture of R1234yf and R32 inside a small-diameter horizontal microfin tube has been obtained. The effects of mass velocity, vapor quality, and saturation temperature on frictional pressure drop were investigated. The results show that the increase in mass velocity enhances the frictional pressure drop, and the frictional pressure drop at saturation temperature of 30 °C is lower than the pressure drop at a saturation temperature of 20 °C at the same experimental conditions. Also, Goto *et al.* (2001)'s correlation has good agreement for all of mass velocity, with average deviation (AD) of -32% and mean absolute deviation (MD) of 32%.

NOMENCLATURE

The nomenclature should be located at the end of the text using the following format:

A	cross sectional area	(m ²)
d	diameter	(m)
G	mass velocity	(kg m ⁻² s ⁻¹)
h	enthalpy	(J kg ⁻¹)
m	flow rate	(kg s ⁻¹)
ΔP	pressure drop	(Pa)
Q	heat exchange amount	(W)
T	temperature	(°C)
v	specific volume	(m ³ kg ⁻¹)
Δv	specific volume difference between saturated vapor and saturated liquid	(m ³ kg ⁻¹)
x	vapor quality	(-)
ΔZ	measuring length	(m)

Greek symbols

γ	apex angle	($^{\circ}$)
ρ	density	(kg m^{-3})
θ	helix angle	($^{\circ}$)
δ	area ratio	(–)
ξ	void fraction	(–)
ϕ	two-phase pressure drop multiplier	(–)
	$\phi = 1 + 1.64 X_{tt}^{0.79}$	
X_{tt}	Martinelli parameter	(–)
	$X_{tt} = \{(1-x)/x\}^{0.9} (\rho_v / \rho_l)^{0.5} (\mu_l / \mu_v)^{0.1}$	

Subscript

c	abrupt contraction
e	abrupt expansion
exp	experimental
eq	equivalent
F	friction
l	liquid
R	refrigerant
pre	predicted
sat	saturation
T	total
v	vapor

REFERENCES

- Constable, G., Somerville, B., (2003). *A Century of Innovation: Twenty Engineering Achievements That Transformed Our Lives*. Joseph Henry Press.
- Del Col, D., Torresin, D., & Cavallini, A. (2010). Heat transfer and pressure drop during condensation of the low GWP refrigerant R1234yf. *International Journal of Refrigeration*, 33(7), 1307–1318. <https://doi.org/10.1016/j.ijrefrig.2010.07.020>
- Diani, A., Cavallini, A., & Rossetto, L. (2017). R1234yf condensation inside a 3.4 mm ID horizontal microfin tube. *International Journal of Refrigeration*, 75, 178–189. <https://doi.org/10.1016/j.ijrefrig.2016.12.014>
- Diani, A., Tamura, M. T., Mancin, S., Barbosa, J., & Rossetto, L. (2014). *2460 Page 1 R1234yf Flow Boiling Heat Transfer Inside a 3.4 mm ID Microfin Tube*. 1–10.
- F. Poggi, H. Macchi-Tejeda, D. Leducq, A. Bontemps, Refrigerant charge in refrigerating systems and strategies of charge reduction, *International Journal of Refrigeration* 31 (2008) 353–370, <https://doi.org/10.1016/j.ijrefrig.2007.05.014>.
- G. Myhre, D. Shindell, F.-M. Bréon, W. Collins, J. Fuglestedt, J. Huang, D. Koch, J.-F. Lamarque, D. Lee, B. Mendoza, T. Nakajima, A. Robock, G. Stephens, T. Takemura, H. Zhang, Anthropogenic and natural radiative forcing, in: T.F. Stocker, D. Qin, G - K. Plattner, M. Tignor, S.K. Allen, J. Doschung, A. Nauels, Y. Xia, V. Bex, P.M. Midgley (Eds.), *Clim. Chang. 2013 Phys. Sci. Basis. Contrib. Work. Gr. I to Fifth Assess. Rep. Intergov. Panel Clim. Chang*, Cambridge University Press, Cambridge, UK, 2013: pp. 659–740. doi:10.1017/CBO9781107415324.018.
- Goto, M., Inoue, N., & Ishiwatari, N. (2001). Condensation and evaporation heat transfer of R410A inside internally grooved horizontal tubes. *International Journal of Refrigeration*, 24(7), 628–638. [https://doi.org/10.1016/S0140-7007\(00\)00087-6](https://doi.org/10.1016/S0140-7007(00)00087-6)
- Hirose, M., Ichinose, J., & Inoue, N. (2018). Development of the general correlation for condensation heat transfer and pressure drop inside horizontal 4 mm small-diameter smooth and microfin tubes. *International Journal of Refrigeration*, 90, 238–248. <https://doi.org/10.1016/j.ijrefrig.2018.04.014>
- John G. Collier and John R. Thome. (1994). *Convective Boiling and Condensation Third Edition*.
- Khairul Bashar, M., Nakamura, K., Kariya, K., & Miyara, A. (2020). Development of a correlation for pressure drop of two-phase flow inside horizontal small diameter smooth and microfin tubes. *International Journal of*

- Refrigeration*, 119, 80–91. <https://doi.org/10.1016/j.ijrefrig.2020.08.013>
- McLinden, MO, Kazakov Andrei, F, Brown, JS, Domanski, P, 2014. A thermodynamic analysis of refrigerants: possibilities and tradeoffs for low-GWP refrigerants. *International Journal of Refrigeration* 38, 80–92.
- McLinden, M. O., & Huber, M. L. (2020). (R)Evolution of Refrigerants. *Journal of Chemical and Engineering Data*, 65(9), 4176–4193. <https://doi.org/10.1021/acs.jced.0c00338>
- Oruç, V, Devecio ğlu, AG, Ender, S, 2018. Improvement of energy parameters using R442A and R453A in a refrigeration system operating with R404A. *Appl. Therm. Eng.* 129, 243–249.
- Vuppiladadiyam, A. K., Antunes, E., Vuppiladadiyam, S. S. V., Baig, Z. T., Subiantoro, A., Lei, G., Leu, S. Y., Sarmah, A. K., & Duan, H. (2022). Progress in the development and use of refrigerants and unintended environmental consequences. *Science of the Total Environment*, 823, 153670. <https://doi.org/10.1016/j.scitotenv.2022.153670>

ACKNOWLEDGEMENT

The Japan Copper Development Association financially supported this study. We wish to express our gratitude for their financial support. The author also would like to express special appreciate to MEXT Saga University for the Master Scholarship.

APPENDIX

Table 1: The experimental and predicted frictional pressure drop

G [kgm ⁻² s ⁻¹]	x [-]	The experimental frictional pressure drop	The predicted frictional pressure drop
50	0.141	0.079	0.060
	0.207	0.123	0.117
	0.346	0.201	0.157
	0.408	0.245	0.190
	0.496	0.287	0.218
	0.610	0.343	0.257
	0.701	0.376	0.281
	0.803	0.402	0.301
	0.898	0.418	0.318
100	0.950	0.420	0.321
	0.124	0.336	0.330
	0.225	0.565	0.500
	0.325	0.771	0.665
	0.435	1.133	0.807
	0.537	1.440	0.937
	0.646	1.717	0.998
	0.740	1.837	1.067
	0.836	1.935	1.131
	0.900	1.895	1.147
200	0.973	1.875	1.118
	0.089	1.196	0.650
	0.219	1.930	1.188
	0.295	2.526	1.700
	0.423	3.846	2.093
	0.525	4.619	2.497
	0.629	5.344	2.592
	0.737	6.057	2.771
	0.838	5.974	2.857
0.925	5.523	2.887	